Journal of Colloid and Interface Science 364 (2011) 1–9

Contents lists available at SciVerse ScienceDirect

Journal of Colloid and Interface Science

www.elsevier.com/locate/jcis

Editor's Choice

Highly transparent and conductive thin films fabricated with nano-silver/double-walled carbon nanotube composites

Shie-Heng Lee, Chih-Chun Teng, Chen-Chi M. Ma *, Ikai Wang

Department of Chemical Engineering, National Tsing-Hua University, Hsin-Chu 30013, Taiwan, ROC

ARTICLE INFO

Article history:
Received 15 June 2011
Accepted 11 August 2011
Available online 22 August 2011

Keywords:
Carbon nanotube
Transparent conductive film
Electrical resistance
Flexible
Nano-silver

ABSTRACT

This study develops a technique for enhancing the electrical conductivity and optical transmittance of transparent double-walled carbon nanotube (DWNT) film. Silver nanoparticles were modified with a $NH_2(CH_2)_2SH$ self-assembled monolayer terminated by amino groups and subsequent surface condensation that reacted with functionalized DWNTs. Ag nanoparticles were grafted on the surface of the DWNTs. The low sheet resistance of the resulting thin conductive film on a polyethylene terephthalate (PET) substrate was due to the increased contact areas between DWNTs and work function by grafting Ag nanoparticles on the DWNT surfaces. Increasing the contact area between DWNTs and work function improved the conductivity of the DWNT-Ag thin films. The prepared DWNT-Ag thin films had a sheet resistance of 53.4 Ω/sq with 90.5% optical transmittance at a 550 nm wavelength. After treatment with HNO_3 and annealing at 150 °C for 30 min, a lower sheet resistance of 45.8 Ω/sq and a higher transmittance of 90.4% could be attained. The value of the DC conductivity to optical conductivity (σ_{DC}/σ_{OP}) ratio is 121.3.

1. Introduction

Transparent conductive thin films (TCF) are widely used in electronic devices, such as touch screen panel [1,2], solar cell [3], thin film transistors [4], and field emission displays [5,6]. These applications usually use indium tin oxide (ITO) films due to their high electrical conductivity and optical transparency [7,8]. However, ITO thin films can seriously limit flexible TCF applications. Increasing the bending angle of the ITO film drastically increases the original sheet resistance of the film [9,10]. Another drawback to applying ITO films in TCFs is that ITO often requires high processing temperatures and can be very brittle. Therefore, replacing ITO film with mechanically flexible and cost-effective materials that can form films under practical conditions is necessary.

A suitable substitute for ITO is poly(3,4-ethylenedioxythiophene):poly (4-stryrenesulfonate) (PEDOT:PSS), which is a conductive polymer system. Flexible films prepared with PEDOT:PSS possess conductivity that exceeds 60% strain [11]. However, the low transparency and conductivity [12] of PEDOT:PSS restricts its usefulness in many practical applications.

When conventional transparent electrodes make use of another material in place of ITO, they need to have a sheet resistance of less than 100 Ω/sq, optical transparency of ~90%, and unlimited scalability. DC conductivity to optical conductivity (σ_{DC}/σ_{OP}) ratio of materials shall be greater than 35 (optical conductivity can be got from the optical absorption coefficient) [13]. Silver nanowire networks, graphene thin films and carbon nanotube (CNT) thin film can overcome many of the shortcomings inherent in ITO and can be highly conductive with good transparency and extreme flexibility [14–17].

Silver nanowire thin films can be prepared by a variety of techniques which obtains a sheet resistance of 13 Ω/sq, optical transparency 85%, and DC conductivity to optical conductivity ratio is 500 [15]. One of the most recently reported methods, vacuum filtration [15] involves dispersion using a porous mixed cellulose ester filter membrane and subsequent transfer to a PET substrate using heat and pressure. However, the vacuum filtration technique requires that silver nanowire films are first formed on filter paper, making large-scale coatings difficult. Another problem with silver nanowire films is their adhesion to PET. Unlike carbon nanotube thin films, silver nanowire thin films failed the adhesion test because they were completely removed from the substrate [15]. In the dropped technique [16], a volume of the nanowire suspension is dropped on a glass substrate with pre-patterned silver contact pads that are 100 nm thick, and the film is subsequently annealed at 200 °C for 20–40 min. The higher temperature also results in a poor candidate for thermally sensitive flexible substrates.

Recently, Bae et al. [17] discovered and demonstrated roll-to-roll production of graphene films for transparent conductive films. Graphene grown on copper foil by a CVD system at 1000 °C. After growth, the graphene film on copper foil is attached to a thermal release tape by applying soft pressure between rolls. The graphene

* Corresponding author. Address: National Tsing-Hua University, Department of Chemical Engineering, Hsin-Chu 30013, Taiwan, ROC. Fax: +886 3 5715408.
E-mail address: ccma@che.nthu.edu.tw (C.-C.M. Ma).

0021-9797/$ - see front matter © 2011 Elsevier Inc. All rights reserved.
doi:10.1016/j.jcis.2011.08.029

film on the thermal release tape is transferred to a target substrate by the rollers. The graphene film has a sheet resistance as low as 30 Ω/sq with 90% transparency. However, the roll-to-roll production requires the graphene thin films to be formed on copper foil first and transferred to the target substrate. This batch-to-batch production is complicated and limited to commercial products and applications.

Carbon nanotube thin film can overcome many of these shortcomings and can be highly conductive with good transparency and extreme flexibility [18]. CNT films can be prepared by a variety of techniques [19,20], and the most recently reported methods are vacuum filtration [21,22] and dip-coating [23]. However, the vacuum filtration technique requires the CNT films to be first formed on a filter, making it difficult to implement coating on a large scale. The dip-coating technique needs to be repeated with the substrate up to 10–100 times in order to optimize the film surface for conductive application. Therefore, the need exists to develop a technique that allows for practical implementation of CNT coatings that is scalable, coat-effective and suitable for roll-to-roll printing. In addition, the electrical conductivity of pure CNT thin films (using only CNTs to prepare thin film without adding any metal particles or conductive polymers) is not as good as individual CNTs. The relatively high sheet resistance of CNT thin films is attributed to large tube-tube contact resistance between CNTs [16]. This problem may be addressed by using DWNTs grafted with metal nanoparticles, which provide dense nanoscale contact regions that enable continuous and well formed contact surfaces.

This study develops a simple and convenient process to fabricate DWNT-Ag transparent conductive thin films. Briefly, this process includes five steps: (1) oxidation of DWNTs with a mixture of sulfuric acid and nitric acid to introduce negatively charged carboxylic groups to the DWNTs surface. (2) A surface condensation method followed by preparation of aligned assemblies of Ag nanoparticles on the DWNTs surface. This step immobilized, amino-terminated Ag nanoparticles on carboxylic DWNT surfaces using a condensation reaction between the carboxyl and amino groups with the aid of dicyclohexylcarbodiimide (DCC) [24,25]. (3) DWNT-Ag thin films were coated on the polyethylene terephthalate (PET) substrate using wet coating techniques (wire-wound rod coating). (4) The DWNT-Ag thin films were immersed in a HNO_3 and ultrasonicated for 10 s [26]. (5) The DWNT-Ag thin films were then annealed at 150 °C in air for 30 min. Due to their size, the Ag nanoparticles melted at 150 °C, increasing the contact area between DWNTs [27,28]. This enhancement in the contact area between DWNTs improved the conductivity of the DWNT-Ag thin films. The annealing process also reduced the sheet resistance of the DWNT-Ag thin films.

2. Experimental section

Oxidizing DWNTs with a single or mixture acid is a well-known chemical treatment for carbon nanotubes. However, oxidizing carbon atoms at the caps generated defects in the sidewalls of the CNTs. Researchers have used this oxidation method to produce short CNTs [29] and functionalize DWNTs [30,31].

2.1. Preparation of functionalized DWNTs suspensions

The CNTs used in this study were DWNTs (purchased from Xinnano Materials, Inc., Taiwan). The DWNTs were functionalized by chemical oxidation in concentrated sulfuric acid and nitric acid, generating —COOH groups at the open end of the tubes. The DWNTs were then boiled at 90–100 °C in a H_2SO_4/HNO_3 (3:1) mixture [29,32] for 1 h.

The reaction mixture was then diluted with deionized water (DI water) and allowed to stand overnight for precipitation. The supernatant was decanted, and the remains were diluted with DI water and filtered with a poly-tetrafluoroethylene (PTFE) membrane with 0.5 μm diameter pore under vacuum. DWNTs sample were obtained by washing the supernatant on the PTFE filter with DI water until the pH of the DWNTs were nearly neutral. The functionalized DWNTs were dispersed in ethanol and sonicated for 1 h without any surfactants.

2.2. Preparation of nano-silver colloids

Silver nitrate, used as a precursor of Ag, was dissolved in ethylene glycol (EG) with 1% polyvinylpyrrolidone (PVP), which was used to prevent the aggregation of Ag nanoparticles [33]. A silver nitrate solution (0.5 mM, 100 mL) was added to the hot PVP-EG solution at a reaction temperature of 120–150 °C. The mixture was stirred vigorously for 30 min. after the reaction was completed, the suspension was cooled to room temperature, and the silver nanoparticles were separated from the PVP-EG solution by centrifugation and washed with DI water to remove the EG and PVP. The resulting particles were dispersed in ethanol while sonicated at 1500 W for 1 h.

2.3. Preparation of mono-dispersed Ag nanoparticles on DWNTs surfaces

The functionalized DWNTs were dispersed in ethanol (ca. 0.5 mg/mL) and sonicated for 1 h. A certain amount of DCC (ca. 0.8 mg/mL) was added into the DWNT suspension and the mixture was ultrasonicated for 30 min. The $H_2N(CH_2)_2S$—Ag was prepared by reacting 100 mL nano Ag colloids (ca. 51 μM) with $H_2N(CH_2)_2SH$ (30 mM in ethanol) at 80 °C for 6 h. The $H_2N(CH_2)_2S$═Ag ethanol solution (100 mL) was decanted into 100 mL of the DWNTs suspension, and a surface condensation reaction [34,35] was performed at room temperature for 24 h. Finally, DWNT-Ag samples were obtained by filtering and washing the remaining solvent on a PTFE filter with DI water.

2.4. Preparation of Ag-DWNTs transparent conductive thin films

Fig. 1 shows the schematic diagram of DWNT-Ag transparent conductive thin film formation steps by wire-wound rod coating method. (A) The DWNT-Ag powder was ultrasonically dispersed in solution, and (B) the suspension of DWNT-Ag was coated on the PET substrate using the bar-coating method. The DWNT-Ag was distributed over the PET film surface, (C) dried in an oven to remove the solvent, and (D) annealed, resulting in DWNT-Ag network thin films. Annealing caused the Ag nanoparticles on the DWNTs surfaces to melt, increasing the contact area between DWNTs. The DWNT-Ag powder (10 mg) was dispersed in a mixture of 35 mL DI water and 15 mL isopropyl alcohol (IPA) which contained 0.5 wt.% SDS. The DWNT-Ag suspension was probe sonicated for 10 min at 1500 W and centrifuged at 13,450*g* (relative centrifugal force) for 30 min. The supernatant part of DWNT-Ag suspensions were selected for making conductive film. The coating rod was placed on top of the PET substrate, and the DWNT-Ag coating suspension was added behind the rod. The rod was then drawn down the substrate to obtain a DWNT-Ag thin film, which was dried immediately in air at 100 °C for 5 min.

2.5. Pos-treatment of DWNT-Ag transparent conductive thin films

The DWNT-Ag powder was dispersed with SDS in a mixture of DI water and IPA. The DWNT-Ag solution was coated on the PET substrate with a coating bar and baked at 100 °C for 5 min. The

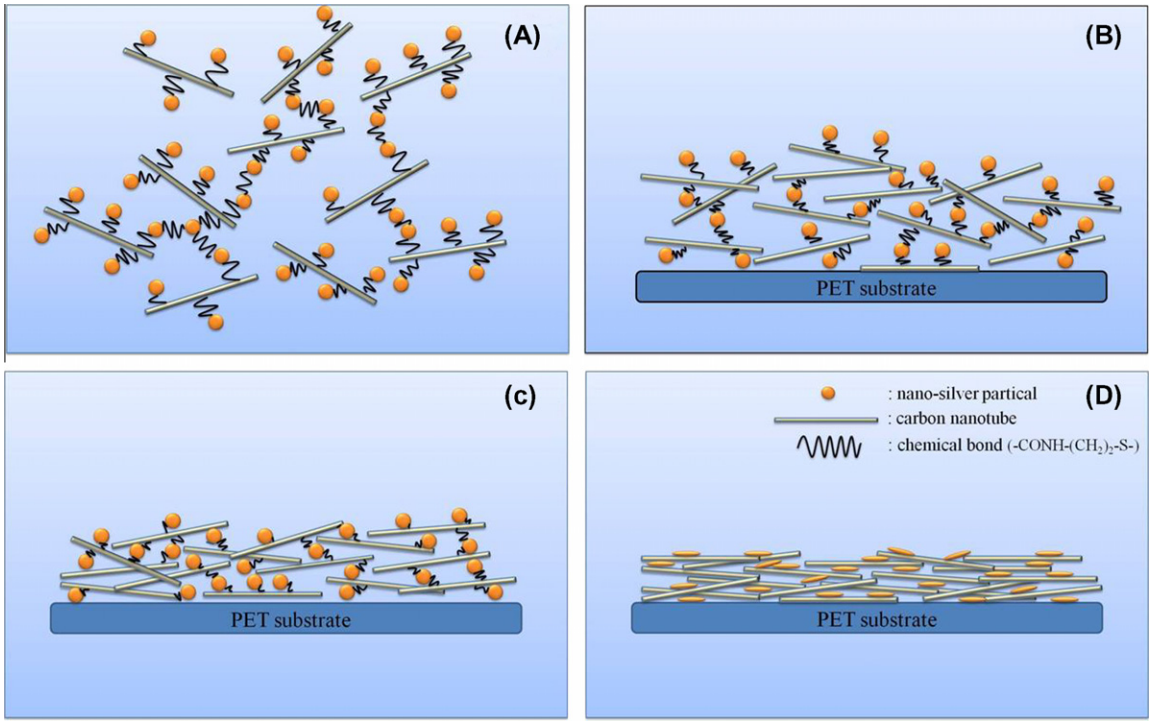

Fig. 1. the schematic diagram of DWNT-Ag transparent conductive thin film formation steps: (A) in solution, (B) wet Ag-DWNTs film on the PET substrate, (C) dried Ag-DWNTs film, and (D) annealed films.

DWNT-Ag thin films were immersed in 5 M HNO_3 solution under ultrasonication at low energy (50 W, 120 kHz) for 10 s to remove the SDS in the DWNT-Ag network [26]. In the subsequent process, the DWNT-Ag thin films were annealed at 150 °C for 30 min. The Ag nanoparticles melted at 150 °C, increasing the contact area between DWNTs to reduce the sheet resistance of DWNT-Ag thin films.

2.6. Characterization

X-ray photoelectron spectra (XPS) measurements were performed using a VG Scientific ESCALAB 220 iXL Spectrometer equipped with a hemispherical electron analyzer and an Mg Kα ($h\nu$ = 1487.7 eV) X-ray source. Transmission electron microscopic (TEM) measurements were taken with a JEM-2100 microscope operating at 200 kV. Scanning electron microscopic (SEM) images were obtained using a (JEOL) JSM-5300 scanning electron microscope. The samples for TEM measurements were prepared by drop casting solution on carbon-coated copper grids and solvent evaporation at room temperature in air. A UV–Vis spectrophotometer (Shimadzu, UV-2501PC) measured the optical transmission profile between wavelength of 200 nm and 800 nm. The sheet resistance (R_s) was characterized using a four-pin probe meter (Loresta EP, MCP-T360) with a working range of 10^{-3}–10^{7} Ω/sq.

3. Results and discussion

3.1. Conductive behaviors

A model is proposed to explain the conductive behavior in TCFs as shown in Fig. 2. There are two main factors control the charge transport across the surface of this thin film: (1) the intrinsic resistance of DWNTs (R_{tube}), (2) the high tube to tube contact resistance between individual DWNT comprising the network ($R_{tube-tube}$) [23].

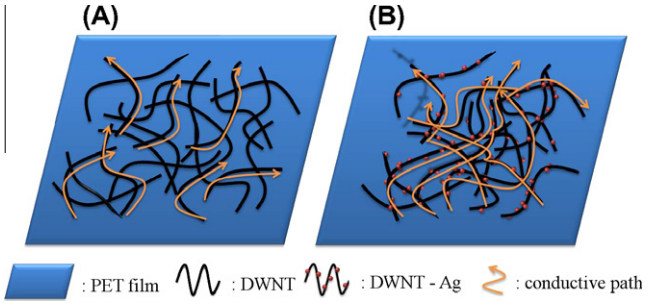

Fig. 2. Illustration of the films without Ag nanoparticles will break the conductive paths (A), and the film with Ag nanoparticles which possesses good conductivity paths (B).

Thess et al. [36] reported that the resistivity of individual single-walled carbon nanotubes was 0.34–1 μΩ m. They also measured the resistivity of single-walled carbon nanotube networks (not transparent CNT network) was 60 μΩ m [37]. When they further improved the contact between single-walled carbon nanotubes and the electrode, the resistivity of single-walled carbon nanotube networks was reduced to 20 μΩ m. These results indicated that the resistivity of single-walled carbon nanotube networks was not as good as individual single-walled carbon nanotube; these could be due to the high contact resistance between CNTs [38,39]. This problem could be addressed by decorating with Ag nanoparticles. Ag nanoparticles act as useful nanospacer and conductor, which not only increases the interlayer spacing (increase the contact probability between tube to tube and tube to Ag) but also improves the electrical conductivity between tubes (increase the work function of DWNT-Ag). DWNTs grafted with Ag nanoparticles providing dense nanoscale contact regions that enable continuous and well formed contact surfaces. The Ag nanoparticles decorated on each side of DWNTs provide conductive paths between DWNTs.

The work function is the minimum energy necessary to pull an electron at the Fermi Level to a point an infinite distance away outside the surface. The work function is an important parameter to consider when a junction with a metal is involved. A precise knowledge of the electronic structure at a CNT/metal junction is necessary for using CNTs. The contact resistance between the metallic materials and the DWNTs, controlled by the Schottky barrier, was significantly decreased compared to the pristine DWNTs. The decrease in contact resistance is attributed to the 0.39 eV increase of the work function of the Ag-DWNTs.

3.2. Morphology of Ag nanoparticles grafted on DWNTs

Fig. 3 illustrates the basic methodology for immobilizing Ag nanoparticles on DWNT surfaces using a condensation reaction. DWNTs were oxidized with a mixture of sulfuric acid and nitric acid in order to introduce carboxylic groups on the DWNTs surface, as shown in Fig. 3A. Ag nanoparticles were modified with self-assembled monolayers of $NH_2(CH_2)_2SH$, resulting in $H_2N(CH_2)_2S$—Ag groups (Fig. 3B). The functionalized DWNTs possessing carboxyl groups on the surface reacted with the amino groups on the silver surface through amide bonds. Using DCC as a coupling reagent, the Ag nanoparticles were grafted on the DWNT surfaces *via* amides bonds, as shown in Fig. 3C.

Transmission electron microscopy (TEM) reveals the morphologies and sizes of the Ag nanoparticles. Fig. 4 shows an image of silver nanoparticles obtained by reducing 100 mL of 0.5 mM $AgNO_3$ with a hot ethylene glycol (EG) solution at 120–150 °C. This TEM image reveals the Ag products, which show the existence of fine spherical nanoparticles. The Ag nanoparticles had diameters ranging from 5 to 10 nm.

TEM analysis also revealed the surface morphology and distribution of Ag nanoparticles on the DWNT surface. Fig. 5 show TEM images of Ag nanoparticles grafted on the DWNT surfaces. The Ag nanoparticles have a distinct circular morphology and grafted on the DWNT surfaces. Covalent bonding of carboxyl-terminated groups on the DWNT surfaces provided a uniform surface [40] after the condensation reaction with amino-terminated Ag nanoparticles. Adding a coupling reagent resulted in the grafting of Ag nanoparticles to the DWNT surface. Fig. 5A–D presents TEM images of DWNTs that were reacted with Ag nanoparticles

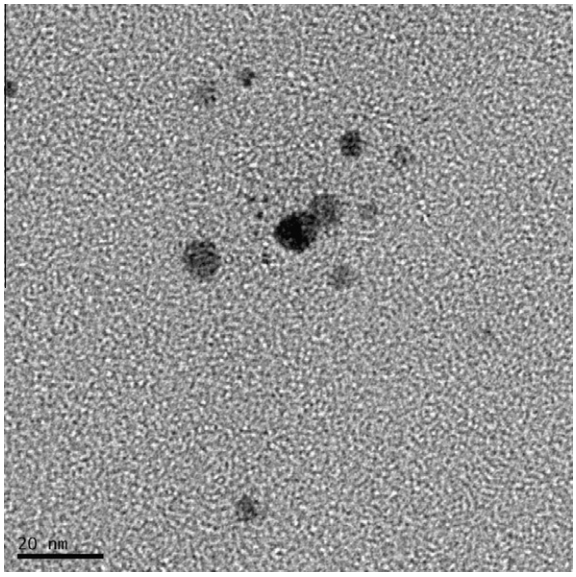

Fig. 4. TEM images of silver nanoparticles obtained by reducing $AgNO_3$ with a hot EG solution.

solution of different concentrations: (A) 48 mM, (B) 121 mM, (C) 164 mM, and (D) 312 mM. The colloidal silver concentration was evaluated by conductometric titration with a 1.0×10^{-3} M HNO_3 aqueous solution. Increasing the concentration of Ag colloids resulted in the grafting of more Ag nanoparticles on the DWNT surface.

3.3. XPS spectra of Ag-DWNTs hybrid structures

The Ag-DWNTs hybrid structures were further analyzed using XPS. Fig. 6 presents a survey spectrum of the hybrid nanostructures, showing strong signals for Ag, C, O, N, and S. The C signal with a binding energy of 285 eV is from the DWNTs and corresponds to the C 1s core level, as shown in Fig. 6A. The O signal with a binding energy of 532 eV (in Fig. 6B) is from the Ag-DWNTs and corresponds to the O 1s core level; the presence of oxygen

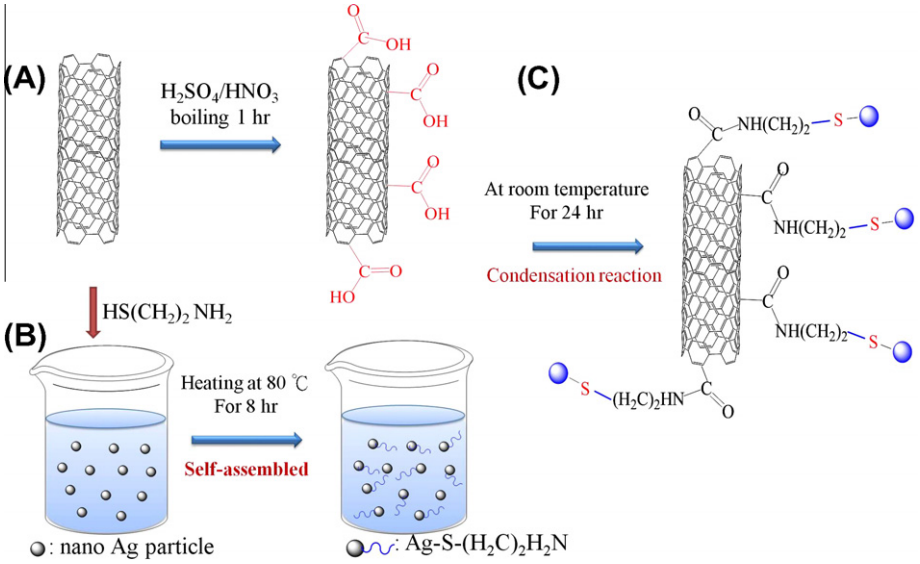

Fig. 3. The basic methodology of immobilizing silver nanoparticles on DWNTs surfaces through amidation. (A) Oxidizing DWNTs with the mixture of acids, (B) modifying the silver surface with $NH_2(CH_2)_2SH$, and (C) amide-forming reaction.

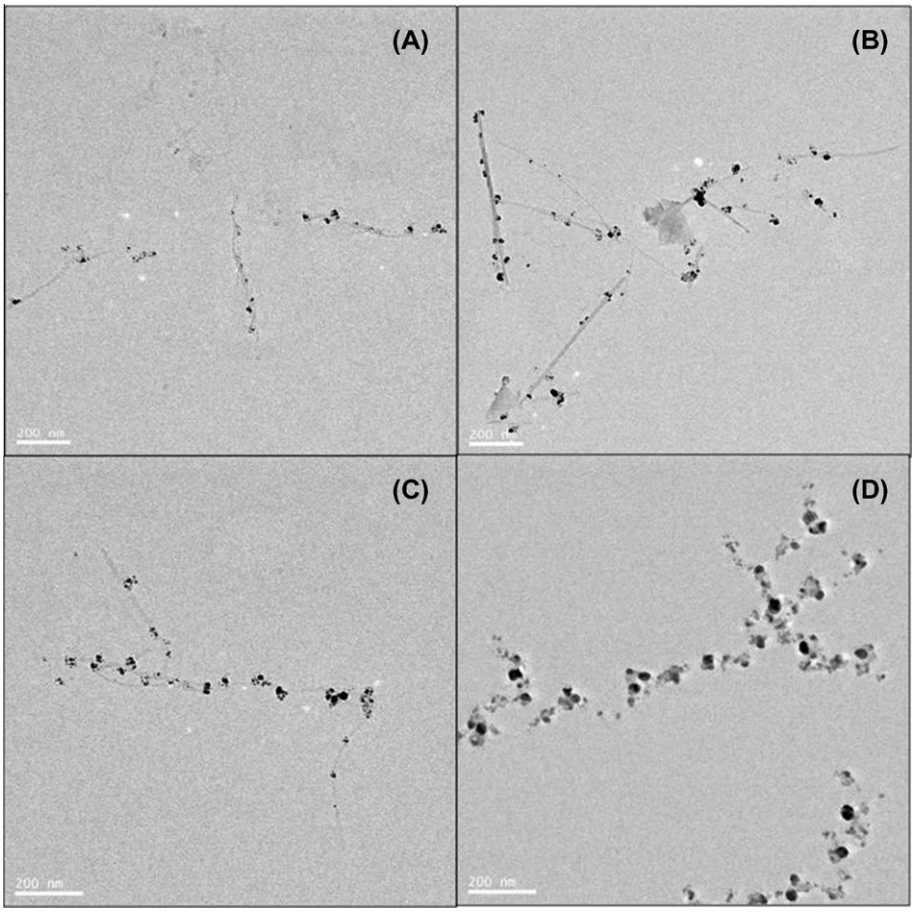

Fig. 5. TEM images of DWNTs reacted with different amounts of Ag colloids (A) 48 mM, (B) 121 mM, (C) 164 mM and (D) 312 mM.

indicates that the pristine DWNTs were modified with carboxylic groups *via* oxidation in acid. The signals corresponding to S 2p, N 1s, Ag $3d_{5/2}$, and Ag $3d_{3/2}$ had binding energies of 53 eV, 401 eV, 369 eV and 375 eV, respectively; these elements originated from the amino-terminated Ag nanoparticles ($NH_2(CH_2)_2S$═Ag), confirming that the amidation reaction was successful.

A detailed analysis of the XPS spectrum provides clear evidence that the Ag-DWNTs were chemically modified. Fig. 7 shows that the carbon C 1s peak at 284.5–285.5 eV corresponds to the combination of the sp^2 C═C and sp^3 C—C structures of the unmodified DWNTs. Another weak peak at approximately 290.9 eV is due to the "shake-up" satellite (π–π^* transition) of DWNTs and intermediate contributions [41]. Three signals with binding energies higher than 285 eV appear in the C 1s spectrum after the surface condensation reaction. The broad signal at 288.5 eV is related to the amide carbon [42]. The existence of a significant amount of C—NH_x indicates that $NH_2(CH_2)_2SH$ functionalized nanoparticles are covalently grafted on the DWNTs surface [43,44]. According to previous research [44,45], the signal with a binding energy of 285.2 eV is due to carbon sulfur bonds (C—S, 285.2 eV).

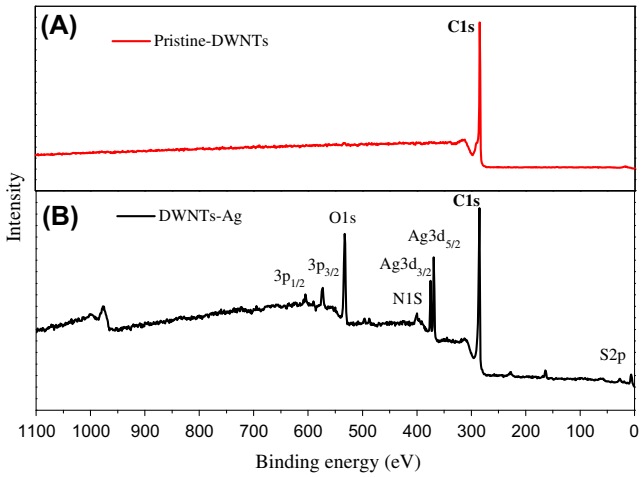

Fig. 6. XPS survey spectrum of (a) pristine DWNTs, and (B) Ag-DWNTs.

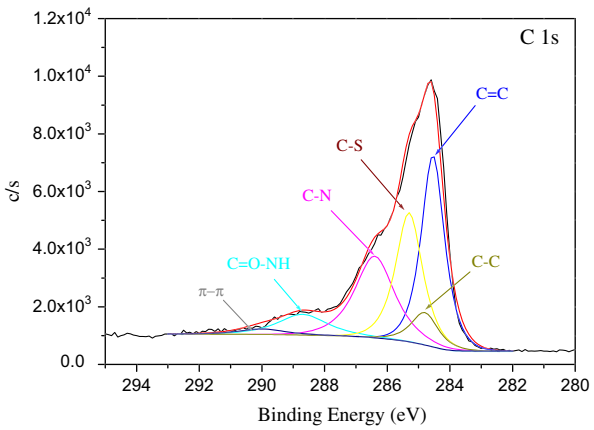

Fig. 7. XPS core level spectra of C1s of Ag-DWNTs.

The Ag 3d doublet appearing at 374.2 eV (Ag $3d_{3/2}$) and 368.2 eV (Ag $3d_{5/2}$) corresponds to silver metal [46,47]. Fig. 8 shows the XPS Ag 3d of the Ag-DWNTs. The binding energies of the Ag $3d_{3/2}$ and $3d_{5/2}$ doublet shift from 374.2 and 368.2 eV to 375 and 369 eV, confirming that Ag nanoparticles were grafted on the DWNT surface *via* silver bonding to sulfur (Ag—S) [48].

3.4. Transparency and sheet resistance properties of DWNT-Ag thin films

Fig. 9 shows the optical transmittance of different Ag-DWNTs thin films as a function of sheet resistance. The percentage of optical transmittance (% *T*) at 550 nm was used to gauge the change in film thickness. Various amounts of Ag colloids that reacted with carboxyl-terminated DWNTs and were grafted to the surface of DWNTs were used to control the sheet resistance and the optical transmittance.

Fig. 9A–D shows the relationship between transmittance and the sheet resistance for different concentration of Ag colloids. Ag nanoparticles grafted on the DWNT surfaces increase the contact area between DWNTs and improve the conductivity of DWNT thin films. With more Ag nanoparticles grafted on the DWNT surface, lower sheet resistances could be attained. However, if too many Ag nanoparticles were grafted on the DWNT surfaces, the conductive thin film had lower sheet resistances and decreased transmittance properties. The conductive films prepared with excess Ag colloids achieved a very low sheet resistance of 28.2 Ω/sq. However, its optical transmittance decreased to 48.18%, as Fig. 9D shows. The DWNT conductive thin films containing Ag nanoparticles grafted on the DWNT surface exhibited lower sheet resistance than those without Ag nanoparticles. AS seen in Fig. 9E, the sheet resistance of the thin films prepared with a neat DWNT suspension (no Ag nanoparticles grafted on the DWNTs surface) was 2.3×10^3 and 8.1×10^4 Ω/sq at an optical transmittance of 91% and 96%, respectively. These data indicated that simultaneously reducing the sheet resistance and obtaining good optical transmittance while still increasing the thickness of the DWNT films is difficult. This observation could be due to the face that the conductivity of the DWNT network was not as good as the DWNT-Ag network.

The transmittance spectrum was shown in Fig. 10, which was the rightmost point of the curve A, B, C and D in Fig. 9. The DWNT-Ag (48 mM Ag colloid, blue curve), thin film had a sheet resistance of 1236 Ω/sq with 93.48% optical transmittance; the DWNT-Ag (121 mM Ag colloid, green curve), thin film had a sheet resistance of 53.4 Ω/sq with 90.5% optical transmittance; the DWNT-Ag (164 mM Ag colloid, red curve), thin film had a sheet resistance of 58.8 Ω/sq with 75.98% optical transmittance; and

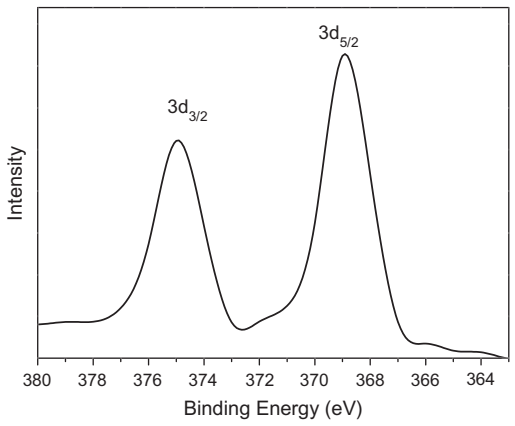

Fig. 8. XPS spectra of Ag 3d core level of DWNTs grafted with Ag nanoparticles.

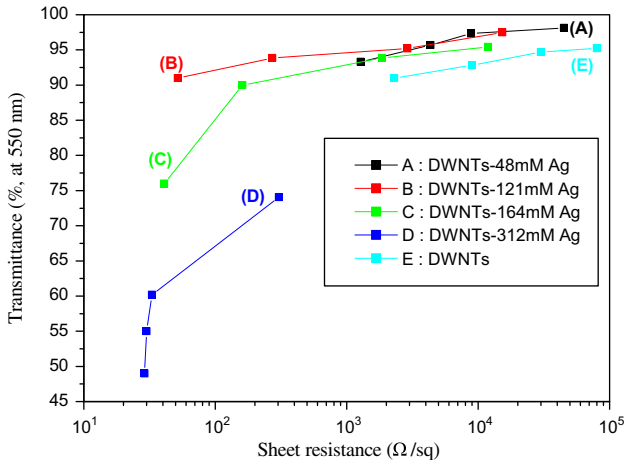

Fig. 9. Optical transmittance of different DWNTs-Ag thin films as a function of sheet resistance.

the DWNT-Ag (312 mM Ag colloid, black curve), thin film had a sheet resistance of 28.2 Ω/sq with 48.18% optical transmittance.

Eq. (1) models the transparency *T* of a thin metallic film in air, assuming that the film thickness is much less than wavelength [49,50]:

$$T = \left(1 + \frac{2\pi}{c}\sigma_{ac}t\right)^{-2} = \left(1 + \frac{z_0}{2R_S}\frac{\sigma_{OP}}{\sigma_{DC}}\right)^{-2} \quad (1)$$

where σ_{DC} is the DC conductivity, σ_{OP} is the optical conductivity, *c* is the speed of light, and Z_0 is the characteristic impedance of vacuum [49] (Z_0 = 377 Ω [50]) both σ_{DC} and σ_{OP} are fundamental properties of a material. A high value of σ_{DC}/σ_{OP} signifies a materials with high conductivity and low optical absorption and hence a better candidate for transparent conductive thin film. Eq. (1) obtains the value of the σ_{DC}/σ_{OP} ratio, fitted by the data of *T* versus R_s for TCF. The σ_{DC}/σ_{OP} ratio fitted are 5.3 (DWNT – 48 mM Ag), 121.3 (DWNT – 121 mM Ag), 40.4 (DWNT – 164 mM Ag), and 21.7 (DWNT – 312 mM Ag). The line are fitted to Eq. (1) for the sheet resistance $<10^5$ Ω/sq. In this study, the optimal concentration of Ag reacted with DWNTs was 121 mM, and it exhibited a higher σ_{DC}/σ_{OP} ratio than other concentration of Ag reacted with DWNTs.

Sodium dodecyl sulfate (SDS) can be washed off easily by immersion in a HNO_3 solution [51]. Remaining SDS significantly degraded the sheet conductance because of its highly insulating

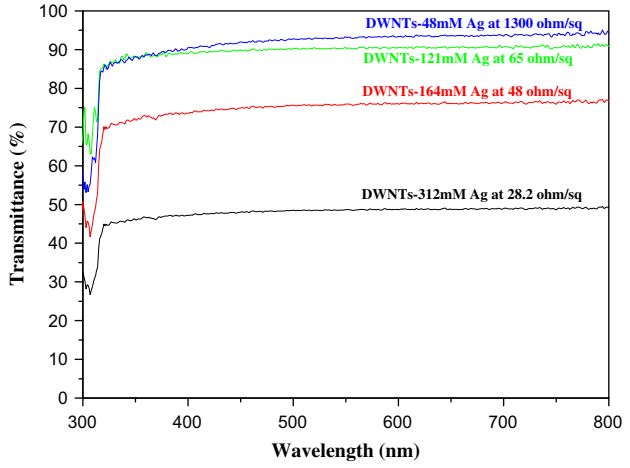

Fig. 10. UV–Vis spectra of DWNT films reacted with different amounts of Ag colloids.

Table 1
Sheet resistance for various transparent DWNT-Ag films.

No	Specimen	Sheet resistance (Ω/sq)			[d]$\Delta\sigma_1/\sigma_0$ (%)	[e]$\Delta\sigma_2/\sigma_0$ (%)	Transmittance (%, at 550 nm)		
		Initial[a] (σ_0)	After HNO_3[b] (σ_1)	After annealing[c] (σ_2)			Initial	After HNO_3	After annealing
1	DWNTs – 48 mM Ag	1236	1104	1052	10.68	14.89	93.48	93.86	93.46
2	DWNTs – 121 mM Ag	53.4	48.6	45.8	8.99	14.23	90.5	90.79	90.4
3	DWNTs – 164 mM Ag	40.8	38.8	36.6	4.90	10.29	75.98	76.56	76.48
3	DWNTs – 312 mM Ag	28.2	27.4	26.3	2.84	6.74	48.18	48.54	48.5

[a] Initial sheet resistance of DWNTs-Ag thin film.
[b] The sheet resistance of DWNTs-Ag thin film after HNO_3 treatment.
[c] The sheet resistance of DWNTs-Ag thin film after an annealing process at 150 °C for 30 min.
[d] $\Delta\sigma_1 = \sigma_0 - \sigma_1$.
[e] $\Delta\sigma_2 = \sigma_0 - \sigma_2$.

nature [26]. HNO_3 can efficiently remove the residual SDS from the DWNTs. The sheet resistance and transmittance data after HNO_3 treatment implies that a considerable amount of SDS was removed by acid treatment because the conductivity and transmittance was significantly improved. After immersing the DWNT-Ag thin films in a 5 M HNO_3 solution, the films were ultrasonicated at 50 W/120 kHz for 10 s to remove the SDS from the DWNT-Ag network. With respect to DWNT-Ag thin films of different Ag concentrations,

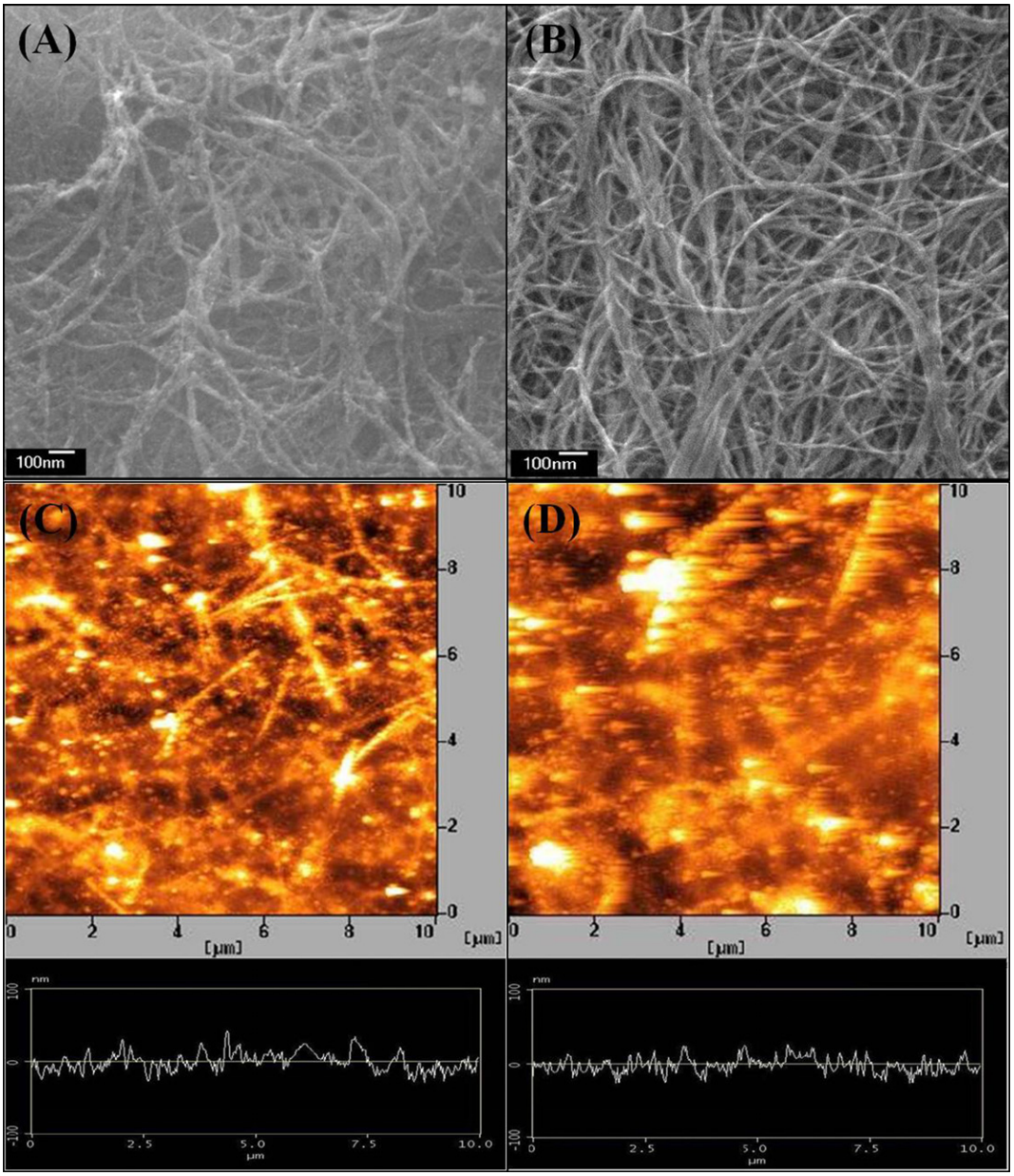

Fig. 11. SEM and AFM images (A and C) and after annealing (B and D).

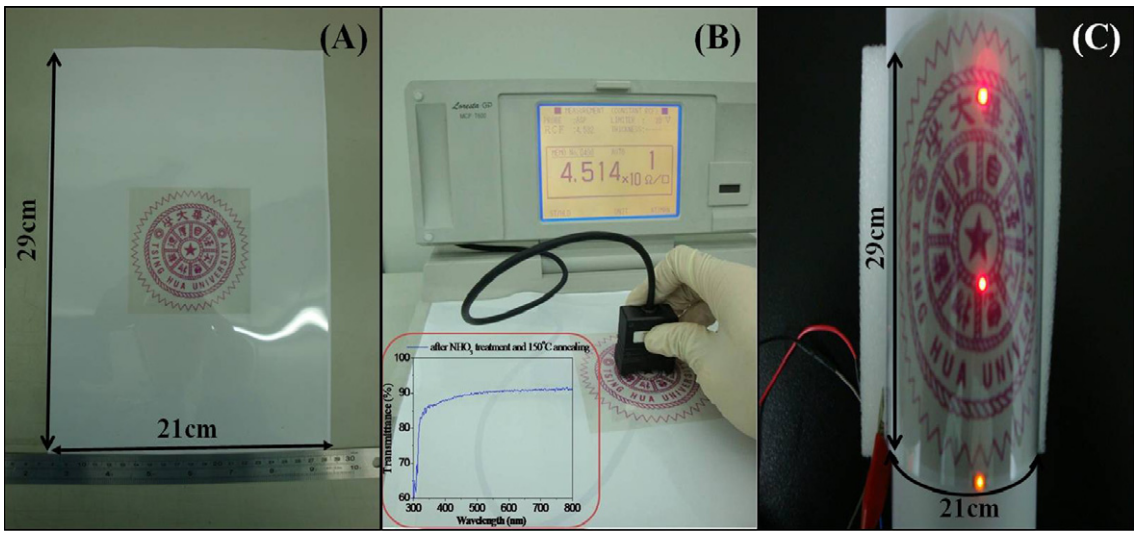

Fig. 12. Images of the DWNT-Ag transparent conductive film coated on a PET substrate (21 cm × 29 cm) (A), the sheet resistance of 45.14 Ω/sq that was measured by a four-pin probe meter (B), and the DWNT-Ag thin film bent 180° with bright LEDs (C).

those treated by HNO_3 exhibited much lower sheet resistance values than those that were not treated with HNO_3, as shown in Table 1. For the thin conductive films treated by HNO_3, a lower sheet resistance of 48.6 Ω/sq could be attained with a higher optical transmittance of 90.79%.

Nanoparticles possess a very high surface-area-to-volume ratio, which provides a tremendous driving force for diffusion, especially at elevated temperatures. Their large surface-area-to-volume ratio also reduces the original melting temperature of nanoparticles [28]. Metal nanoparticles can melt at a relatively low temperature due to their nanometer sizes. The melting temperature of bulk Ag was approximately 960 °C, but the sintering temperature of Ag nanoparticles was lower than 100 °C [27].

The annealing temperature greatly influences the conductivity of the DWNT-Ag film. The initial electrical conductivity (σ_0) was measured, as was the difference between the electrical conductivities of samples before and after annealing ($\Delta\sigma_2$) at 150 °C for 30 min. Table 1 summarizes the main difference in the DWNT-Ag conductivity before and after annealing at 150 °C. The change in sheet resistance before and after annealing at 150 °C ($\Delta\sigma_2/\sigma_0$) is much lower than that associate with increasing the concentration of Ag colloids.

For DWNTs undergoing the condensation reaction with 121 mM Ag colloids (sample 2), the $\Delta\sigma_2/\sigma_0$ was approximately 14.23%. Increasing the concentration of Ag colloids from 48 to 312 mM (sample 4) decreased the $\Delta\sigma_2/\sigma_0$ to 6.74%. This result is due to too many Ag nanoparticles on the DWNT surfaces. When functionalized DWNT reacted with a high concentration of Ag colloids, more Ag nanoparticles were grafted on the tube surface, and the conductivity of DWNT-Ag networks was better than that of DWNTs reacted with less Ag colloids. After annealing at 150 °C for 30 min to decrease the sheet resistance, the sample of DWNTs reacted with higher concentration of Ag colloids (as Table 1 shows for sample 4) did not achieve extra conductive area. The value of $\Delta\sigma_2/\sigma_0$ was lower than that of the sample of DWNTs reacted with lower concentrations of Ag colloids (as shown in Table 1/samples 1–4). Table 1 also presents the transmittance of the Ag-DWNTs film at 550 nm after annealing, which was decreased by only approximately 1%. That is because PET substrate after annealing process appears a little white color changed (very slight) result in the transmittance of DWNT-Ag films decreases. The best results in this study were a sheet resistance of 45.8 Ω/sq and an optical transmittance of 90.4% at a wavelength of 550 nm. Therefore, the sheet resistance and optical transmittance obtained in this study are very competitive for the application of highly conductive, transparent, and flexible displays [52,53].

3.5. Morphology of DWNT-Ag thin films

Fig. 11A shows SEM images of DWNT-Ag thin films (reacted with 121 mM Ag colloids) with a sheet resistance of 53.4 Ω/sq and optical transmittance of 90.5%. The DWNT-Ag films thoroughly and uniformly covered the substrate surface, and there are many Ag nanoparticles grafted on the DWNT surfaces. After annealing at 150 °C for 30 min, we observed a few prominent points on the DWNT surfaces. The surface morphology of DWNT-Ag films was smoother after annealing, as shown in Fig. 11B. After annealing, the DWNT-Ag thin films have a lower sheet resistance of 45.8 Ω/sq and higher optical transmittance of 90.4%. Fig. 11C and D shows AFM images of DWNT-Ag thin films before and after annealing at 150 °C for 30 min. A random network of DWNT-Ag can be observed on the PET surface. The thicknesses of the DWNT-Ag thin films before and after annealing at 150 °C for 30 min are estimated to be 10–50 nm (Fig. 11C) and 10–30 nm (Fig. 11D), respectively.

Fig. 12A shows photographic images of the DWNT-Ag transparent conductive film (functionalized DWNT reacted with 121 mM Ag colloids) coated on a PET substrate (21 × 29 cm). From this image, the film clearly appears to be of high optical transparence with little haze (the haze is 1%). After HNO_3 treatment and annealing at 150 °C for 3 min, a sheet resistance of 45.14 Ω/sq could be attained by a four-pin probe meter, as shown in Fig. 12B. The inset in Fig. 12B shows the UV spectra of DWNT-Ag thin film with sheet resistance of 45.14 Ω/sq. Fig. 12C shows the outstanding flexibility of DWNT-Ag conductive thin film. The DWNT-Ag thin film was divided into positive and negative electrodes by blade cutting, and light-emitting diodes (LEDs) were mounted on the surface of the DWNT-Ag thin film. The DWNT-Ag thin film with LEDs was bent 180° and supplied with power by three 1.5 V batteries. The bright LEDs indicated that the conductive properties of DWNT-Ag thin films would not be affected by extreme bending.

4. Conclusions

This study reports the preparation of highly electrically conductive and transparent thin films from DWNT-Ag suspensions using a

wet coating method. Ag nanoparticles were modified with a $H_2N(CH_2)_2SH$ self-assembled monolayer terminating in amino groups and reacted with functionalized DWNTs. Grafting Ag nanoparticles onto DWNT surfaces significantly increased the performance of the thin conductive films on flexible PET substrates. The DWNT-Ag conductive films (reacted with 121 mM Ag colloids) had a low sheet resistance of 53.4 Ω/sq and optical transmittance of 90.5%. After HNO_3 treatment and annealing at 150 °C for 30 min, the contact area of the DWNT network (DWNT tube-to-tube area) increased because the Ag nanoparticles melts; this change improved the sheet resistance by 14.23%. The resulting DWNT-Ag thin conductive films displayed lower sheet resistances of 45.8 Ω/sq, higher optical transmittance of 90.4%, and the value of the DC conductivity to optical conductivity ratio is 121.3. These materials are potential candidates for flexible applications.

References

[1] S.J. Wang, Y. Geng, Q.B. Zheng, J.K. Kim, Carbon 48 (2010) 1815.
[2] S.L. Hellstrom, H.W. Lee, Z.N. Bao, ACS Nano 3 (2009) 1423.
[3] E.L. Ratcliff, P.A. Lee, N.R. Armstrong, J. Mater. Chem. 20 (2010) 2672.
[4] Q. Sun, J.H. Kim, J.H. Park, S. Seo, Appl. Phys. Lett. 96 (2010) 103301.
[5] S. Vadukumpully, J. Paul, S. Valiyaveettil, Carbon 47 (2009) 3288.
[6] B.J. Yoon, E.H. Hong, S.E. Jee, D.M. Yoon, D.S. Shim, G.Y. Son, J. Am. Chem. Soc. 127 (2005) 8234.
[7] Y. Hu, X. Diao, C. Wang, W. Hao, T. Wang, Vacuum 75 (2004) 183.
[8] X.W. Sun, H.C. Huang, H.S. Kwork, Appl. Phys. Lett. 68 (1996) 2663.
[9] S. Iijima, T. Ichihashi, Nature 363 (1993) 603.
[10] M.S. Dressclhaus, G. Dressclhaus, D.C. Eklund, In Science of Fullerenes and Carbon Nanotubes, Academic Press, New York, 1996.
[11] D.R. Cairns, S.P. Gorkhali, S. Esmailzadeh, J. Vedrine, G.P.A. Grawford, J. Soc. Inform. Disp. 11 (2003) 289.
[12] S. Kirchmeyer, K. Rcuter, J. Mater. Chem. 15 (2005) 2077.
[13] L. Hu, D.S. Hecht, G. Gruner, Nano Lett. 4 (2004) 2513.
[14] A.D. Pasquire, S. Fang, Science 309 (2005) 1215.
[15] D. Sukanta, T.M. Higgins, P.E. Lyon, E.M. Doherty, P.N. Nirmalraj, W.J. Blau, J.J. Boland, J.N. Coleman, ACS Nano 3 (2009) 1767.
[16] J.Y. Lee, S.T. Connor, Y. Cui, P. Peumans, Nano Lett. 8 (2008) 689.
[17] S. Bae, H. Kin, Y. lee, X. Xu, J.S. Park, Y. Zheng, J. Balakrumar, T. Lei, H.R. Kim, Nat. Nanotechnol. 5 (2010) 574.
[18] T. Sreekumar, K. Liu, L. Ericson, R. Hauge, Chem. Mater. 15 (2003) 175.
[19] M. Meitl, Y. Zhou, A. Gaur, S. Jeon, M. Usrey, M. Strano, J. Rogers, Nano Lett. 4 (2004) 1643.
[20] Z. Wu, Z. Chen, X. Du, J.M. Logan, J. Sippel, M. Nikolou, Science 305 (2004) 1273.
[21] Y. Zhou, L. Hu, G. Gruner, Appl. Phys. Lett. 88 (2006) 123109.
[22] Y.I. Song, G.Y. Kim, H.K. Choi, H.J. Jeong, K.K. Kim, C.M. Yang, S.C. Lim, K.H. An, K.T. Jung, Y.H. Lee, Chem. Vap. Deposition 12 (2006) 375.
[23] M.H. Andrew, L.T. Hartadi, H. Tan, C.H. Patrick, Nanotechnology 19 (2008) 205703.
[24] B. Wu, J. Zhang, Z. Wei, S. Gai, Z. Liu, J. Phys. Chem. B 105 (2007) 5075.
[25] X. Nan, Z. Gu, Z. Liu, J. Colloid Interface Sci. 245 (2002) 311.
[26] H.Z. Geng, K.K. Kim, K.P. So, Y.S. Lee, Y. Chang, Y.H. Lee, J. Am. Chem. Soc. 129 (2007) 7758.
[27] Y. Qin, M. Hu, H. Li, Z. Zhang, Q. Zou, Appl. Surf. Sci. 253 (2007) 4021.
[28] P.H. Buffat, J.P. Burrel, Phys. Rev. A 13 (1976) 2287.
[29] J. Liu, A.G. Rinzle, H. Dai, J.H. Hafner, R.K. Bradler, P.J. Boul, A. Lu, R.E. Smalley, Science 180 (1998) 1253.
[30] J. Chen, M.A. Hamon, H. Hu, Y. Chen, A.U. Rao, P.C. Eklund, R.C. Haddon, Science 282 (1998) 95.
[31] J. Chen, M.A. Hamon, S. Lynksyitove, M.E. Itkis, M.A. Hamon, J. Phys. Chem. B 105 (2001) 2525.
[32] S.F. Mckay, J. Appl. Phys. 35 (1964) 1992.
[33] D. Kim, S. Jeong, J. Moon, Nanotechnology 17 (2006) 4019.
[34] Z. Liu, Z.I. Shen, T.I. Zhu, S.J. Hou, L. Ying, Langmuir 16 (2000) 3569.
[35] A. Kudelsji, W. Hill, Langmuir 15 (1999) 3162.
[36] A. Thess, R. Lee, P. Nikolaev, H. Dai, P. Petit, J. Robert, C. Xu, Y.H. Lee, S.G. Kim, A.G. Rinzler, Science 273 (1996) 483.
[37] J.E. Fischer, H. Dai, A. Thess, R. Lee, N.M. Hanjiani, D.L. Dehaas, R. Smally, Phys. Rev. B 55 (1997) R4921.
[38] M.S. Dresselhaus, G. Dresselhans, K. Sugihare, I.L. Spain, H.A. Goldberg, Graphite fibers and filament, in: M. Cardona (Ed.), Material Science, Springer-Verlag, Berlin, 1988, p. 224.
[39] T.W. Ebbesen, P.M. Ajayan, Nature 358 (1992) 220.
[40] K. Dai, L. Shi, J. Fang, Y. Zhang, Mater. Sci. Eng. A 465 (2007) 283.
[41] Y. Zhu, Y. Pan, H. Xu, C. Xiang, H. Kou, J. Guo, J. Chem. Lett. 36 (2007) 1098.
[42] J.D. Liao, S.P. Lin, Y.T. Wu, Biomacromolecules 6 (2005) 392.
[43] X. He, F. Zhang, R. Wang, W. Lin, Carbon 45 (2007) 2559.
[44] G. Beamson, D. Briggs, High Resolution XPS of Organic Polymers: The Scienta ESCA300 Database, John Wiley & Sons, New York, 1992.
[45] O. Carallieri, L. Oliveri, A. Dacca, R. Parodi, R. Rolandi, Appl. Surf. Sci. 357 (2001) 175.
[46] G.A. Gelves, B. Lin, U. Sundararaj, J.A. Haber, J. Adv. Funct. Mater. 16 (2006) 2423.
[47] V.K. Kaushik, J. Electron Spectrosc. Relat. Phenom. 56 (1991) 273.
[48] J.F. Moulder, P.S. Stickle, P.E. Sobol, K.D. Bomben, A Reference Book of Standard Spectra for Identification and Interpretation of XPS Data.
[49] H. Hu, Y.C. Ni, V. Montana, R.C. Haddon, V. Parpura, Nano Lett. 4 (2004) 507.
[50] S. De, P.J. King, M. Lotya, A. ONeill, E.N. Doherty, Y. Hernandez, Small 6 (2010) 458.
[51] J. Kong, H. Dai, J. Phys. Chem. B 105 (2001) 2890.
[52] S. Paul, D.W. Kim, Carbon 47 (2009) 2436.
[53] H.Z. Geng, K.K. Kim, Y.S. Lee, Y.K. Chang, Y.H. Lee, J. Am. Chem. Soc. 129 (2007) 7785.